

## Pretrigger Circuit for Time-of-Flight Counters

D. Jenkins, J. Haverlack, R. Millner and D. Schutt  
Virginia Tech

and

Elton Smith  
CEBAF

May 4, 1994

This report describes the pretrigger circuit which will accept pulses from the time-of-flight (TOF) counters to generate inputs to the CLAS Level 1 Trigger electronics. The circuit will also generate inhibits for the TOF low level discriminators that provide stop pulses to the high resolution TDCs. These outputs are produced by discriminating analog sums of four tubes on adjacent TOF counters. Here we report on tests of the basic summing and discriminating circuits. A prototype of the pretrigger circuit for a pair of scintillators was built and tested.

### The Pretrigger Circuit

The trigger from the TOF counters will be initiated by events that deposit an energy in the scintillators greater than some preselected value. The time of the event will be determined by a separate commercial discriminator set at a low threshold for precise timing. An overall layout of the TOF electronics which processes these signals is shown in Fig. 1. The photomultiplier-tube (PMT) dynode pulses go to the pretrigger circuit where two signals are produced. One of these signals goes to the Level 1 Trigger and the second is an inhibit pulse which is sent to the inhibit input of the low-level discriminator. The inhibit signal will normally be on, but is turned off when an event is accepted by the pretrigger circuit to enable the discriminator to accept the event. A commercial discriminator will be used for fast timing while custom electronics will be used for energy discrimination in the pretrigger circuit. The anode pulse will also be recorded by an ADC for later analysis. A preliminary design report for the circuit has been released as a CLAS note.<sup>1</sup>

Particles can deposit energy in adjacent TOF scintillators because the trajectory of particles from the target will enter the TOF scintillators at an angle and can intersect two counters. Therefore, pulses from adjacent counters must be summed to obtain a pulse amplitude that is proportional to the total energy deposited in the TOF counters. This summation will be performed by the pretrigger circuit shown in Fig. 2. Sixteen scintillators (32 PMTs) are analyzed in each of the pretrigger circuit boards. The dynode pulses from PMTs on opposite ends of a scintillator are summed with the dynode pulses from an adjacent counter to produce a pulse with an amplitude proportional to the energy deposited in the scintillator pair. The summed pulse is then sent to a discriminator. The threshold of this discriminator can be set

remotely. The discriminator output goes to a one-shot which generates a signal with a width that can also be set remotely. The output of the one-shot is sent to the Level 1 Trigger indicating a "doubles" event, i.e. a hit in either of two adjacent scintillators.

Another output of the one shot is "ORed" with outputs from adjacent counters to generate a pulse that will enable the fast discriminator. The fast discriminator, a LeCroy 2313 CAMAC module, has 16 channels which can be individually inhibited. Two LeCroy modules will be required for sixteen counters, one module for PMTs on one side of the counters and the second module for PMTs on the other side. The purpose of the "ORed" pulse is to get timing information for both counters in the path of a crossing track. When a track deposits enough energy in one counter to pass the pretrigger threshold but not enough energy in the second counter, the fast discriminator of the second will be enabled by the pretrigger signal from the first.

To reduce the number of inputs to the Level 1 Trigger from the TOF system, the "ORed" pulse for the large-angle counters (scintillators 17-48), a "triples" pulse, will be sent to the level 1 trigger rather than the doubles pulse. Since the rates at large angles will be lower than at forward angles, the triples pulses can be used.

## **Prototype**

The pretrigger circuit prototype is shown in the attached schematics, Figs. 3 and 4. The first schematic shows, from the left, dynode input signals terminating in 51-ohm resistors, then entering unity gain buffers (EL2003CJs). Additional input components provide transient protection. The buffer outputs are presented to slowing (integrating) networks, which have a characteristic time constant of about 4.7 nanoseconds (rise time of 10.3 nanoseconds). The time constant can be changed to optimize the circuit response.

Signals from the four channels tested are summed at the input of a CLC401AJP current mode amplifier, which scales a buffer output by a gain of 1.7. Summed and amplified signals are input to a MVL407 discriminator, which produces output if the input exceeds the threshold, VTH. VTH, set by a potentiometer in the prototype, will be controlled by a DAC in the final version.

Dynode signals from detectors D01R and D01L are summed with signals D02R and D02L to produce the first discriminator input. D02R and D02L are summed with D03R and D03L to produce the second discriminator input. D03R, D03L, D04R, D04L form the third discriminator input, etc.

The first discriminator output clocks a flip-flop (MC10H131) to produce a Q high output, which then triggers a programmable delay chip (AD9500BQ). The Q output of the 9500 resets the flip-flop after the delay. Delay settings are accomplished with a DIP switch in the prototype, but will be digitally controlled with a 8-bit word via the VXI bus, in the final version.

Q outputs from the flip-flops are buffered and output as differential ECL signals at the TR connector for cabling to the TRigger processor ("doubles").

A MC10H103 "OR" gate combines outputs from adjacent flip-flops and then drives delay lines (200 ns.). The delay line outputs are terminated and the signals regenerated using ECL receivers connected as Schmitt triggers, the outputs of which are buffered by MC10H101s to produce the "Inhibit" differential ECL signals.

Inputs to the second and fourth delay lines are buffered to produce the "Triples" ECL signals, found at the TRIP connector.

### **Test Arrangement**

Two issues were examined in the test of the module:

- How efficient is the circuit for detecting particles which pass thru adjacent scintillators?
- How does the efficiency depend on position along the scintillators?

The circuit was tested by looking at pulses produced by cosmic rays passing through long counters borrowed from Fermilab.<sup>2</sup> The scintillators, made from Bicron BC-408, were two inches thick, 6 in. wide and 120 in. long. The PMTs were Amperex XP2020, with tube bases constructed at Fermilab. One of the tubes was broken and was replaced by an Amperex XP2262. The gain of the PMTs were balanced to give anode pulses of approximately the same amplitude for a given input. For this test, we used the PMT anode pulses as inputs to the pretrigger circuit.

In order to find the trajectory of a cosmic ray passing through the long scintillators, drift chambers were used in conjunction with two trigger scintillators. The layout of the apparatus is shown in Figure 5. The trigger scintillators, at the top and bottom of the counter assembly, measured 12 x 12 inches square. A 2 inch thick lead block above the bottom scintillator insured that particles passing through the two counters were of high energy. The long scintillators were mounted on rollers so that they could be moved between the trigger counters to measure the response of the scintillators at different positions along their length. The counters were tipped at an angle of 19° to increase the probability of a track passing through both counters.

When pulses from the trigger scintillators were in coincidence, a computer readout of the data was begun. Four drift chambers were used to determine the particle's trajectory. Each chamber had four active regions. The trigger coincidence provided a common start on TDCs that measured the time for electrons from the ionizing cosmic ray to reach the anode wires in the drift chambers.

The electronics associated with the scintillators is shown in Fig. 6. Pulses from each of the four PMT anodes were split into three signals. One signal went to the pretrigger discriminator prototype. Information as to whether or not the discriminator triggered was recorded for each event. The second signal went to an integrating ADC and the third signal went to a scaler (not shown). Data for each event were recorded by a CAMAC data acquisition system with MacVee software on

a Macintosh computer.<sup>3</sup>

## Integration Time

The pulse height of the summed dynode signals depends on position not only because of attenuation in the scintillator but also because pulses from opposite PMTs will arrive at the discriminator at different times. The difference in time is due to differences in path length for the two signals in the scintillator. Fig. 7 shows a computer simulation of the summed pulses from the PMTs at opposite ends of a scintillator. The cables to the discriminator were chosen so that tracks at the center of the counter would produce signals that arrive at the discriminator at the same time. These pulses will sum to produce the pulse shown in Fig 7a. A track one foot from an end of a counter will produce signals that arrive at the discriminator at different times to give the summed pulse shown in Fig. 7b. Here the first pulse to arrive is larger in amplitude than the second pulse because the light of the second pulse has more attenuation in the scintillator. But the maximum pulse height is less than it is for a track at the center because the two pulses are not in time. The difference in amplitude is even more pronounced for a track at a distance of 2.5 ft from the end of the scintillator. This situation, shown in Fig. 7c, has appreciable attenuation for both signals as well as differences in timing. The maximum pulse height differs by 48% for these three cases. A discriminator threshold of 600 mv would produce an output for tracks at the center, but would miss good events at the other two positions. The problem is corrected by integrating the pulse so as to average the pulse over a time corresponding to the time difference of arrival for tracks at the discriminator. Then the discriminator will be less sensitive to the position of the track in the scintillator.

To examine the effect of different integration times, a simulation of the PMT pulses was used to model the response of the summing circuit. The summing circuit with integration is shown in Fig. 8. The 47 pF capacitor provides an integration time of 4.7 ns. The shape of the pulse from the scintillator was recorded by a digital scope. The digital values, at about 2.5 ns intervals, were analyzed in the simulation which used Mathematica to obtain a frequency spectrum by a Fourier transform. After dividing the transformed pulse by the circuit impedance, an inverse Fourier transform was calculated to obtain the time spectrum of the current. Fig. 9 shows the effect of different capacitor values for tracks at different positions along the scintillator. The 47 pF capacitance was chosen for the prototype used in our tests. For this capacitor, the maximum amplitude changes by 20% as the position of the track moves down the scintillator. Smaller variations are expected for larger integration times, but variations will remain because of different attenuations for different positions. A variation of 15% was measured at these three positions for a 200 ns integration time in tests described below.

## Test Analysis

Data were collected in 12-hour runs during which about 30,000 events were obtained. The voltage on the PMTs was adjusted so that the average pulse height for each tube was approximately the same for cosmic rays passing through the center of the

counters. A histogram for the PMTs pulses is shown in Fig. 10. To determine the threshold of the pretrigger discriminator, pulses from the four PMTs were added for each event. Fig. 11 shows the histogram for these summed ADCs when the array was positioned to look at cosmic rays entering the middle of the scintillators. Fig 11a shows the summed pulse heights for all events while Fig 11b shows the summed pulse heights for events associated with a trigger from the pretrigger discriminator. Pulses in these histograms are associated with a track through the counter array, but there was no requirement that the track went through the top and bottom of the counters. The low pulse heights correspond to tracks which cut across a corner of the counters leaving less energy than tracks passing through the top and bottom. These histograms indicate that the discriminator was set at a value corresponding to about half of the pulse height for an event with a track passing through the top and bottom of the scintillators.

The analysis of the data began with a calculation of the trajectory from the TDC values to see if a track could be fitted to the data. The coordinate system for the analysis is shown in Fig. 12. 20% of the events satisfied the requirement of having one good track and were kept for further analysis. Next the  $x$  position of the track at the scintillators was found. The  $z$  position of the track was not measured, but it was constrained to an interval of 12 inches by the trigger counters. A diagram of a typical track is shown in Fig. 13. The circles represent the radial distance between the wire and the track as measured by the TDCs.

The events were divided into three types. An event corresponding to a track through the top and bottom of counter TOF1 was called an F1 event. A track through the top and bottom of TOF2 was an F2 event, and a track through the top of one counter and the bottom of the other was called an F12 event. For each of these events, the discriminator data was examined to see if it had been triggered by the event. Fig. 14 shows the histogram for the summed pulses for each of these three types of events. The peaks for the spectrum of F1 and F2 events is about the same while the peak for the F12 event is lower by about 7% showing that there is some loss of light for tracks crossing the counters.

Histograms of the PMTs for cosmic rays passing near the end of the counter are shown in Figures 15, 16 and 17. Fig. 15 shows the pulse height measured for each of the four PMTs with a requirement that a track passed through the top and bottom of the counter array. As expected, the PMT closer to the cosmic ray track receives a larger pulse. Figure 16 shows the summed pulses for the four PMTs with and without a discriminator requirement. The figure shows that the discriminator responded to all good events. Fig. 17 presents the histograms of the summed pulses for the three different types of events: F1, F2 and F12. In this case the peak in the spectrum is the same for the three types of events.

The attenuation of the pulses through the scintillator is shown in Fig. 18 which gives the pulse height in each of the PMTs for pulses produced at different positions along the length of the scintillator. At a position near an end of the scintillator, the pulse received by the nearby PMT is almost three times the amplitude of the pulse received by the opposite PMT. As the position approaches the center of the

scintillator, the pulses received by the two PMTs become equal in value.

Histograms of the sum of the four PMTs at different positions along the scintillator are shown in Fig. 19. Low energy pulses correspond to tracks which clip the edge of the counters. As the position of cosmic rays moves from an end of the scintillator to the center, the summed pulse height changes by about 20%.

### **Efficiency**

The efficiency for each types of event was defined as:

$$\varepsilon = (\text{Number of events with discriminator trigger}) / (\text{Total number of events})$$

The efficiency of the scintillator was measured at five positions from the center of the scintillator pair to one end. Three different efficiencies were determined at each position. The efficiency for tracks passing through the top and bottom of counter TOF1 is  $\varepsilon_{F1}$ , the efficiency of those in TOF2 is given by  $\varepsilon_{F2}$  and the efficiency for tracks which passed through the top of one counter and the bottom of the other is  $\varepsilon_{F12}$ . The three efficiencies were greater than 99% for all positions measured along the scintillators.

### **Conclusion**

The pretrigger circuit is successful in combining pulses from adjacent scintillators to give high efficiency for cosmic rays at all positions along the scintillator. A similar test should be performed with the scintillators, PMTs and tube bases for the actual counters to be used in the CLAS TOF system, since the efficiency depends on the pulse height produced by the counters.

### **Acknowledgments**

We thank Serge Canizares for his assistance in the early phase of the project, Rick Jones for providing us with advice in using the MacVee system, and Norman Morgan for loaning the drift chambers. We also thank Ed Jastrzembski, Dave Doughty and Peter Bonneau for helpful discussions about the circuit board design, in particular the VME interface.

<sup>1</sup>TOF splitter/Discriminator, Preliminary Design Report, R. Christopher Cuevas, CLAS\_Note 91-024

<sup>2</sup>The scintillators are described in "Design and Performance of a Time-Of-Flight System for Particle Identification at the Fermilab Collider", by Bannerjee et al, Nucl. Inst. Methods A269, 121 (1988).

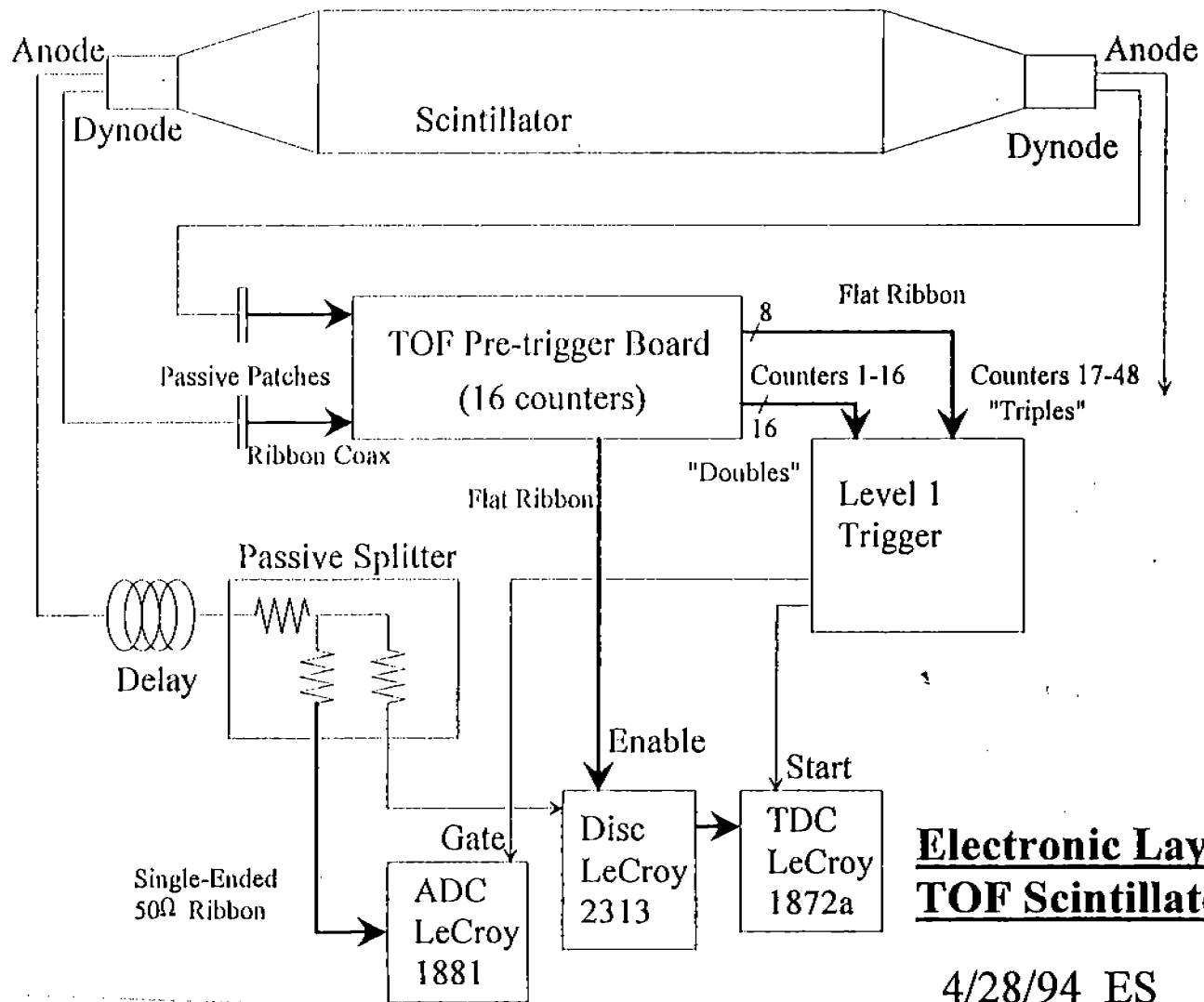
<sup>3</sup>UA01 Technical Note 90-01, CERN.

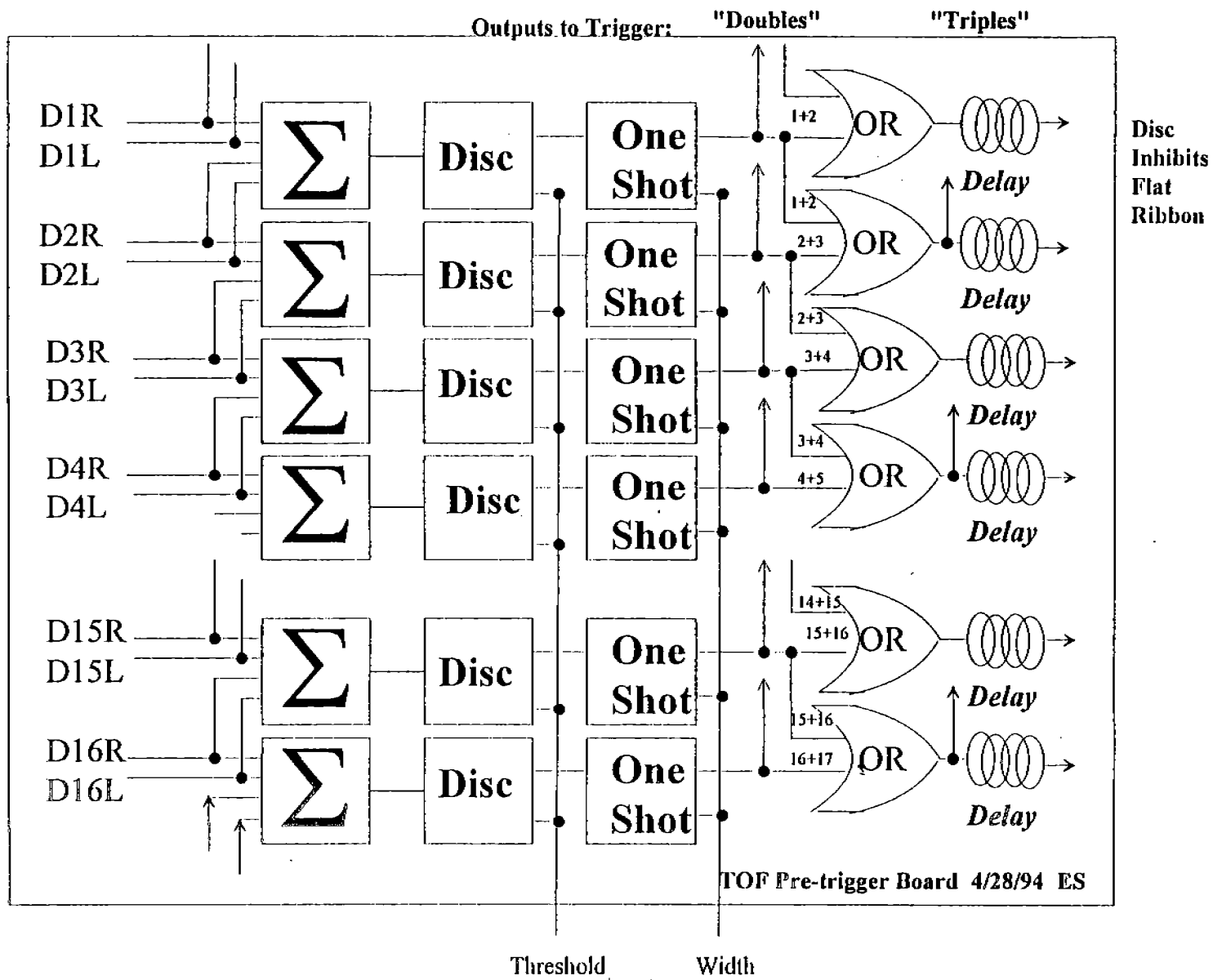
## Figures

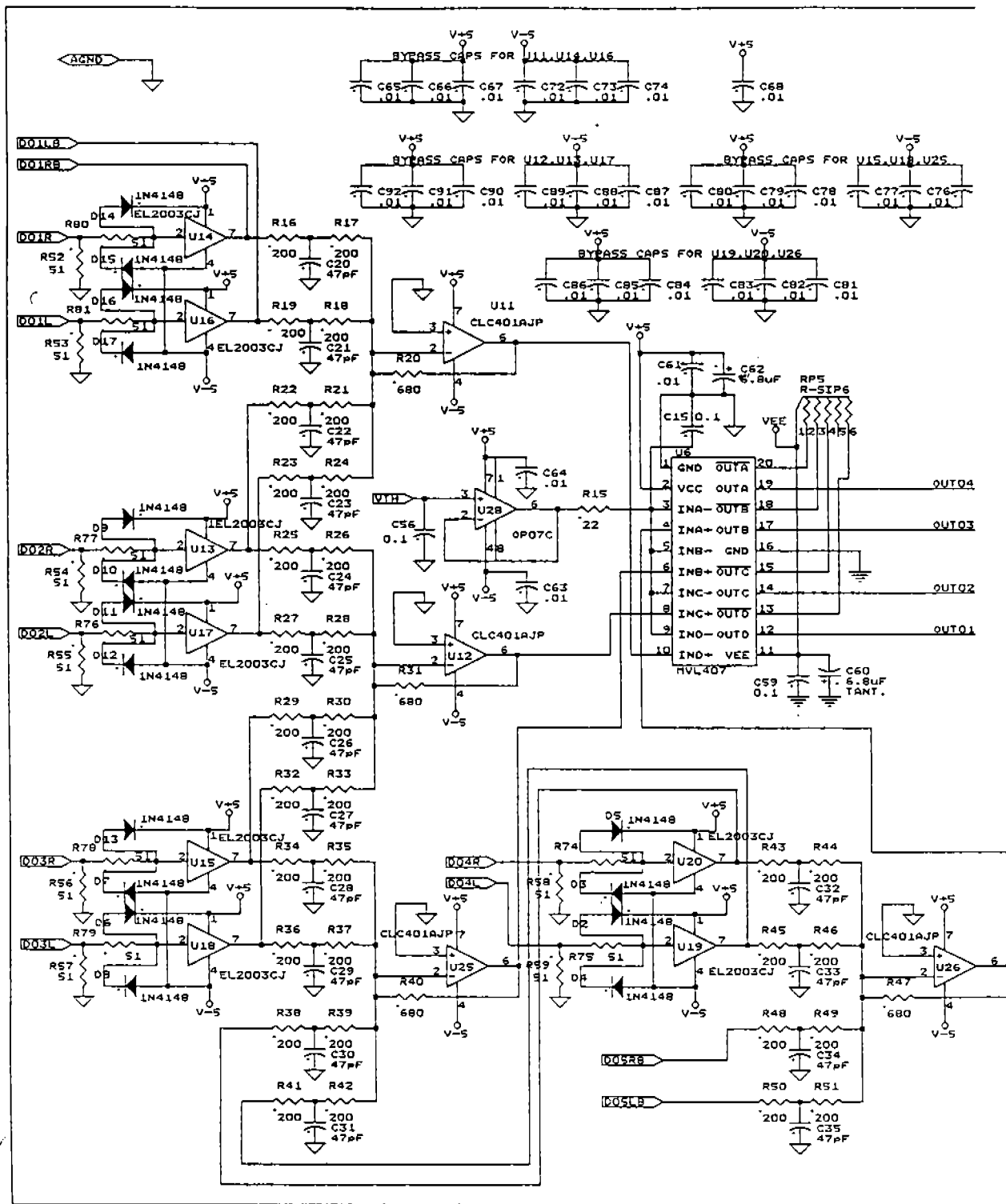
1. Electronics for the time-of-flight counters
2. Logic diagram for the pretrigger circuit
- 3 a, b. Schematic of the pretrigger circuit, Part I. The original drawing has been divided into the two parts of the figure.
4. a, b. Schematic of the pretrigger circuit, Part II. The original drawing has been divided into the two parts of the figure.
5. Counter geometry for test of prototype pretrigger circuit
6. Logic diagram for test of prototype pretrigger circuit.
7. Simulated spectrum of the sum of pulses from PMT's on opposite ends of the scintillator. The top spectrum is produced by a cosmic ray passing through a position 5 feet from one end (center) of the scintillator. The middle spectrum is produced by a cosmic ray 1 foot from an end and the lower spectrum 2.5 feet from the end.
8. Circuit in pretrigger prototype for adding four PMT pulses.
9. Simulated output of summing circuit for different integrating capacitors and different positions of the cosmic ray in the scintillator. The first column represents the summed pulses for a 25 pF capacitor, the second column a 47 pF capacitor and the third column is for 100 pF. The top row shows the pulses for cosmic rays 1 foot from one end, the middle row for cosmic rays 2.5 ft from an end and the bottom row is for a position 5 feet from the end which is at the center of the counter.
10. Histogram of PMT output for events at the center of the scintillator with a track identified by the drift chamber as passing through the top and bottom of the counter. The left and right PMT's on counter TOF1 are designated L1 and R1, respectively. The left and right PMT's on TOF2 are labeled L2 and R2.
11. Histogram of summed PMT pulses with no pretrigger discriminator requirement (top) and with a pretrigger discriminator requirement (bottom). There was no track requirement in the drift chambers for these histograms.
12. Coordinate system for calculating tracks in the drift chamber.
13. Typical track recorded by the drift chambers. The circles show the distance of the track from wires in the four drift chamber planes. The line tangent to the circles was derived by the analysis program which resolved the left-right ambiguity to find the most likely path of the cosmic ray.

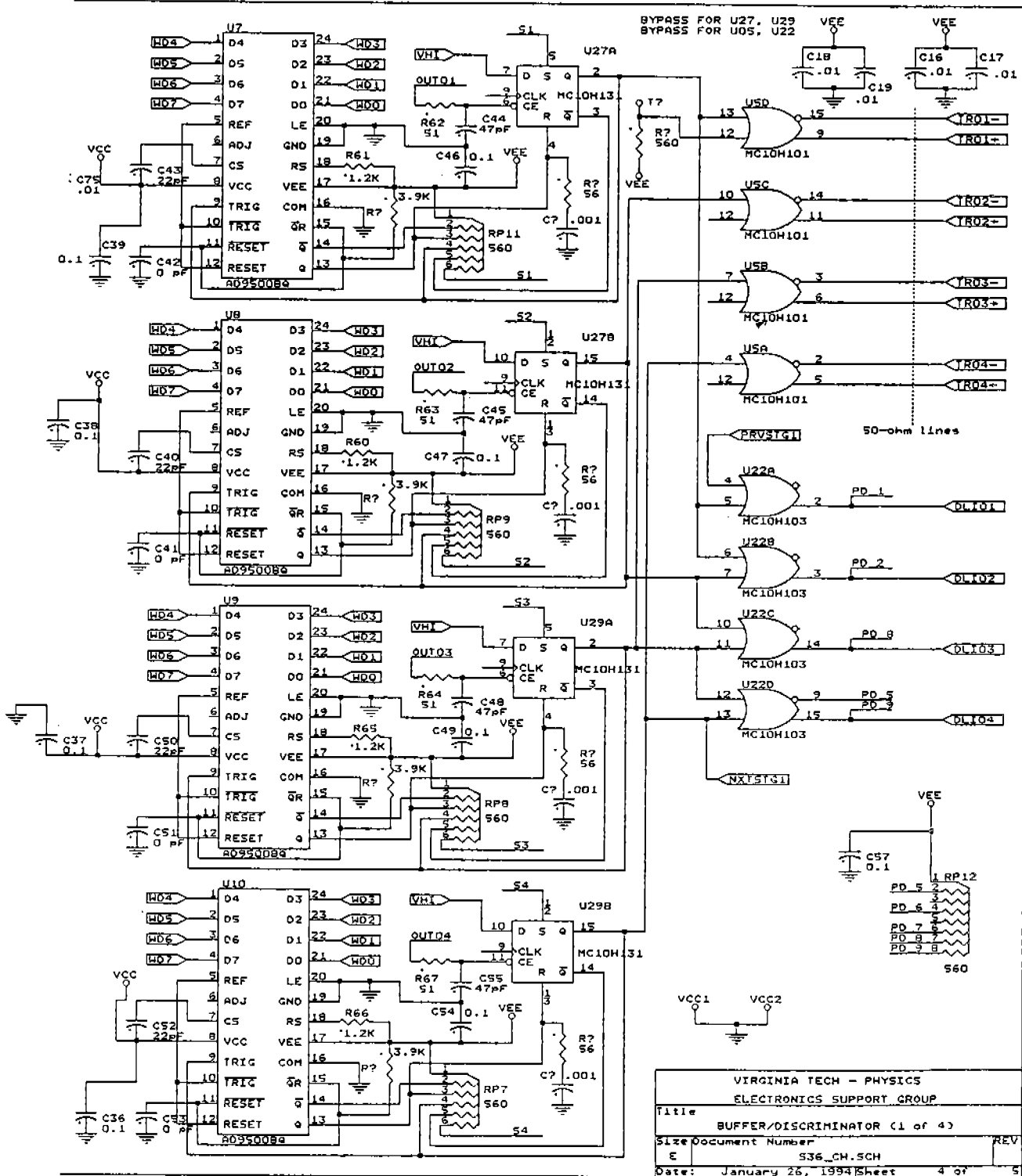


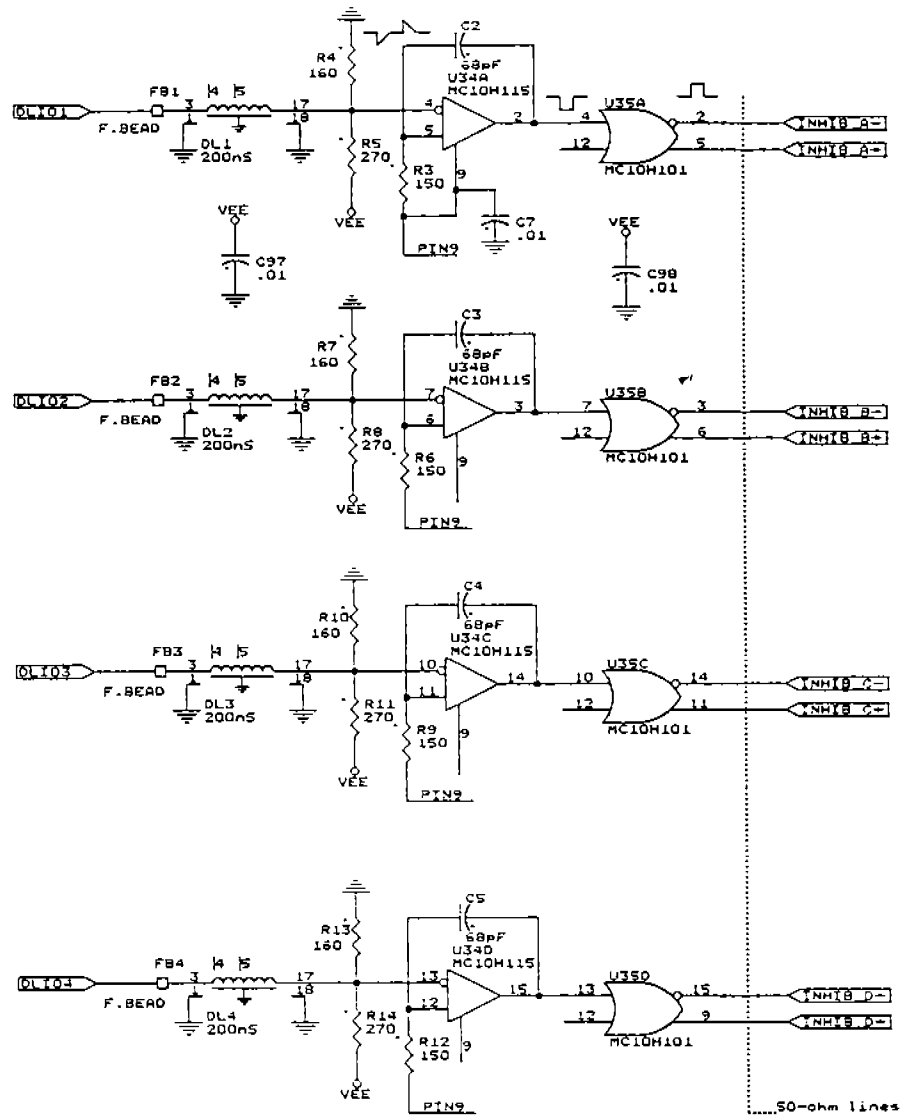
14. Histogram of the summed PMT pulses for tracks passing through the top and bottom of the counters; (a) for counter TOF1, (b) for TOF2 and (c) for a track through the top of one counter and the bottom of the other. A discriminator output was required for each point in the histogram.
15. Histogram of PMT output for cosmic rays one foot from the end of the scintillator. The figure is similar to Fig. 10 for cosmic rays at the center of the scintillator.
16. Histogram of summed PMT pulses for tracks one foot from scintillator end; (a) with no pretrigger discriminator requirement and (b) with a pretrigger discriminator requirement.)
17. Histogram of summed pulses for tracks one foot from scintillator end for which the drift chambers identified the event as (a) type F1, (b) type F2 or (c) type F12. A discriminator output was required for each point in the histograms.
18. The amplitude of PMT signals for tracks at different distances in the scintillator from PMT R1 and R2. PMT's L1 and L2 are at the opposite ends of the scintillators.
19. Histogram of summed PMT signals for tracks at different positions along the scintillator. Small pulses correspond to tracks which did not pass through the top and bottom planes of the scintillators.

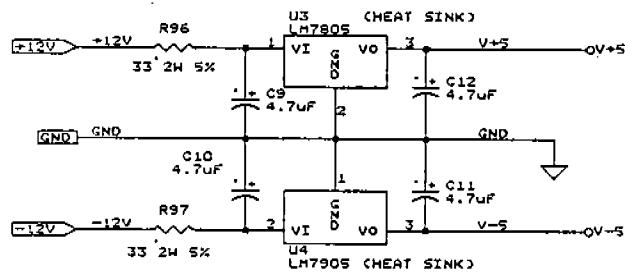
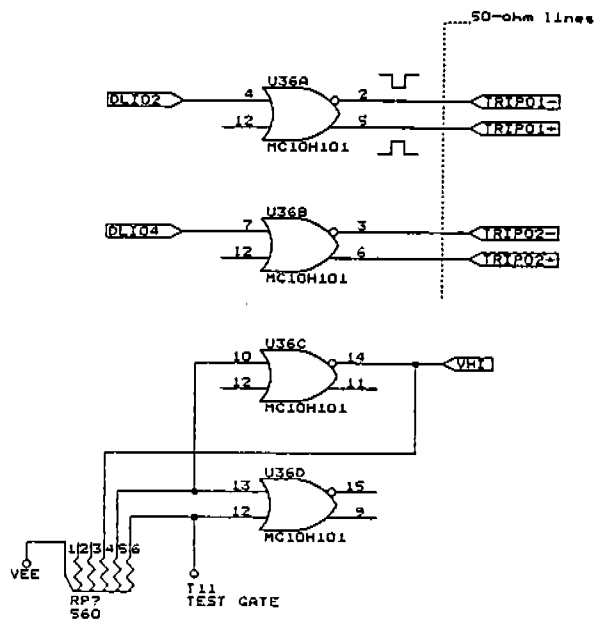






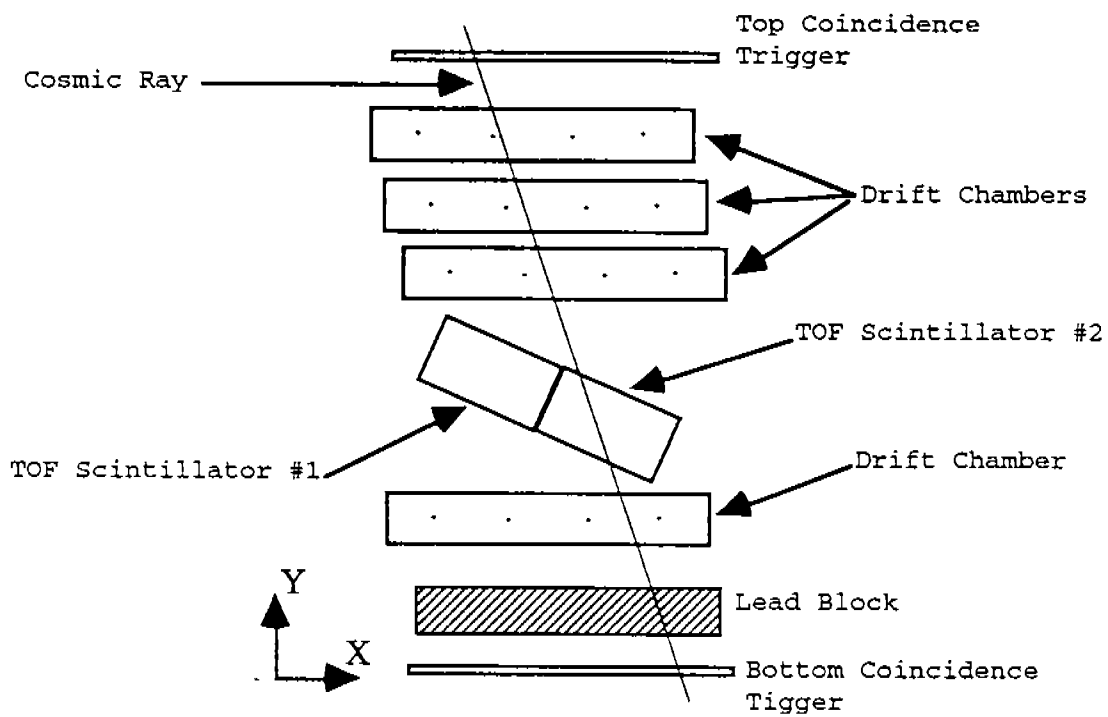




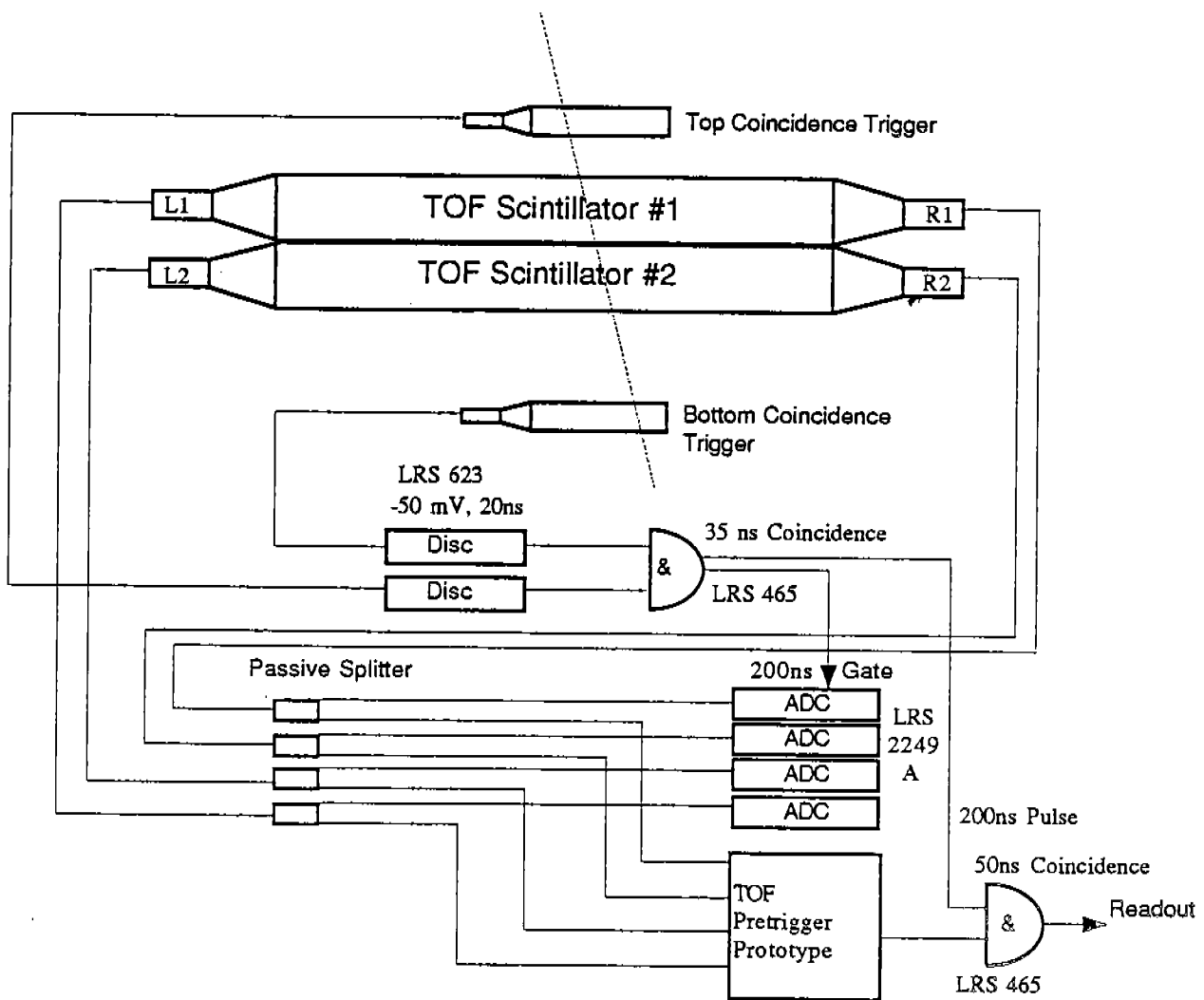


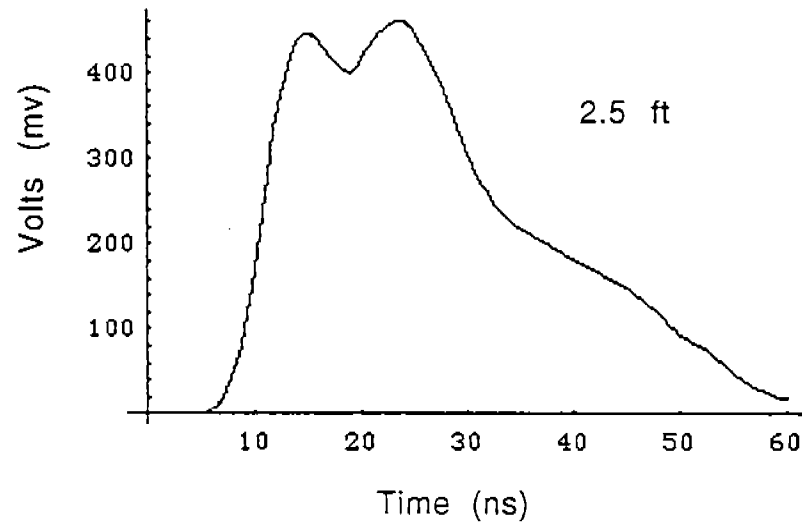
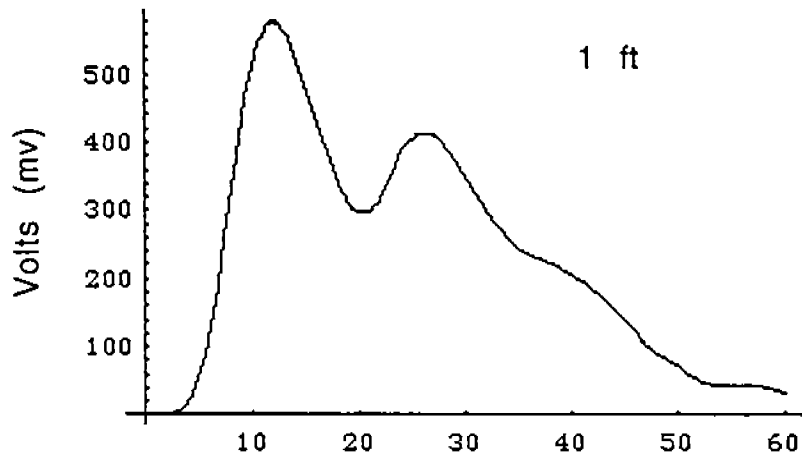
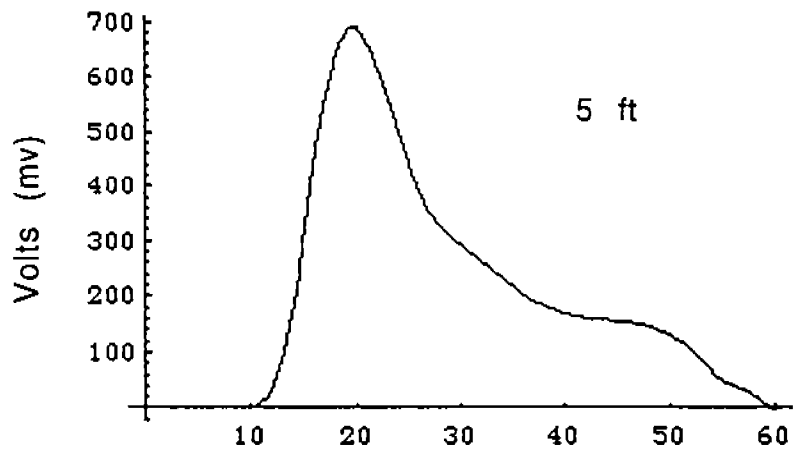
Note: Regulators flat-to-board on heat sinks.

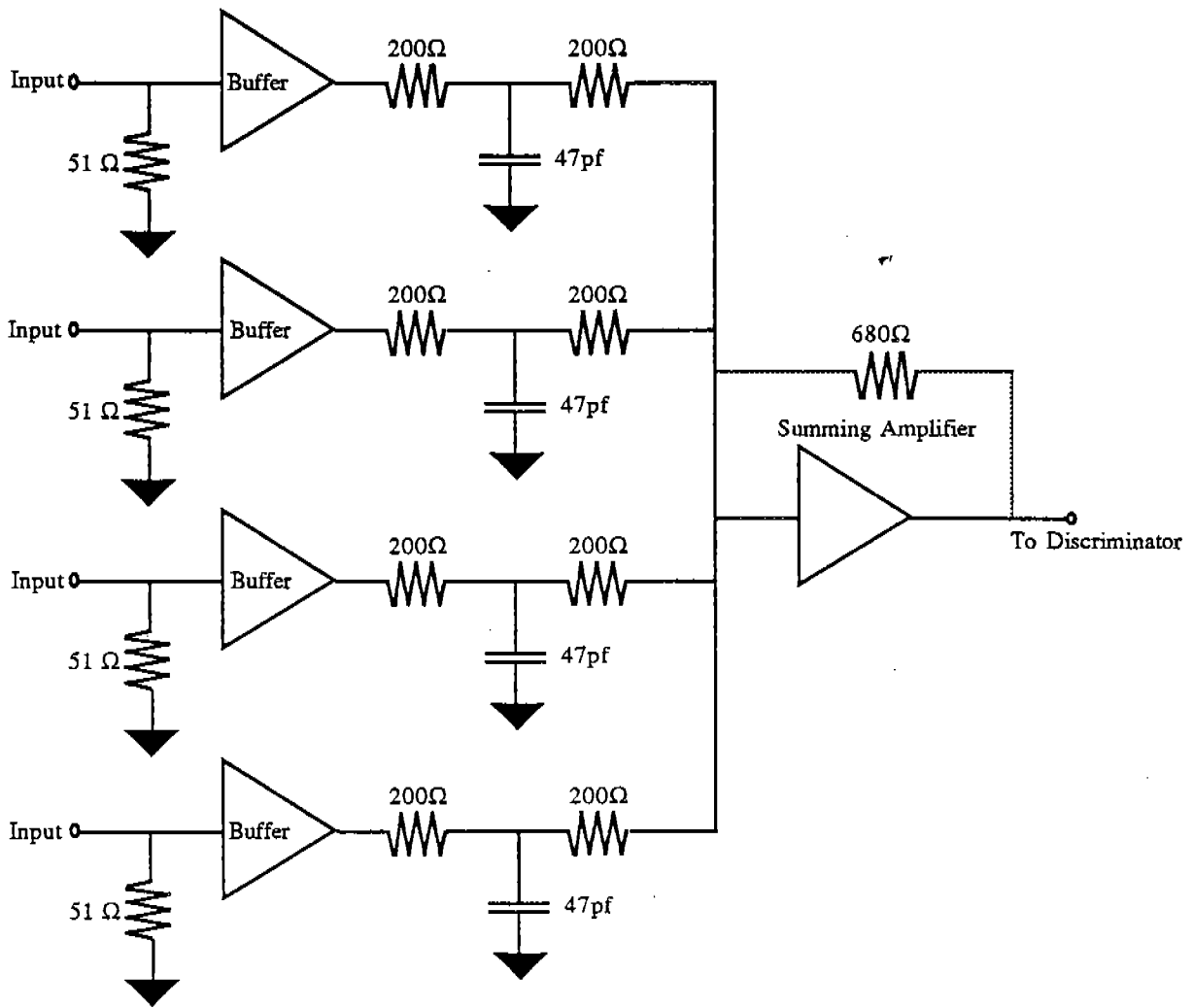
VIRGINIA TECH - PHYSICS	
ELECTRONICS SUPPORT GROUP	
Title	
DL01_04, DELAY LINES, ETC.	
Size Document Number	
E	S36_DL.SCH
Date: January 26, 1994	Sheet 5 of 5



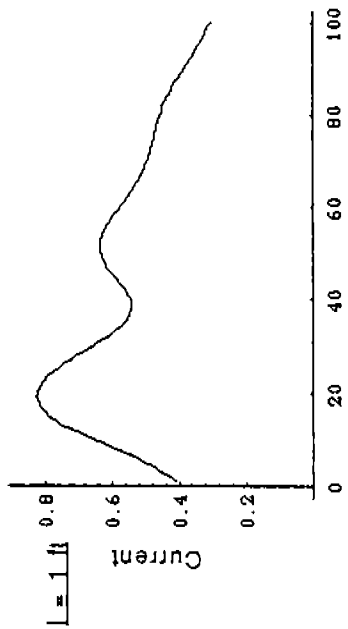








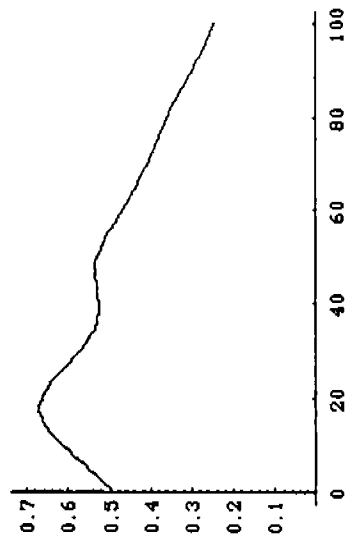
25 pE



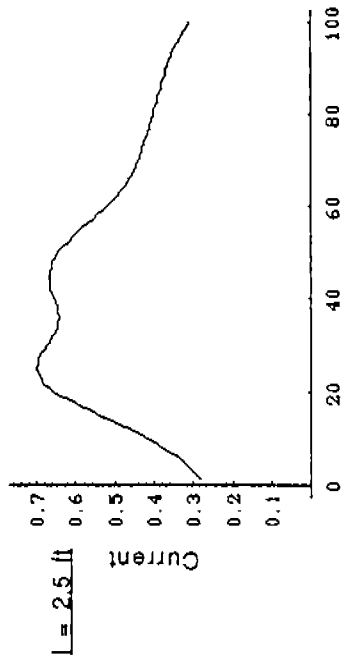
47 pE



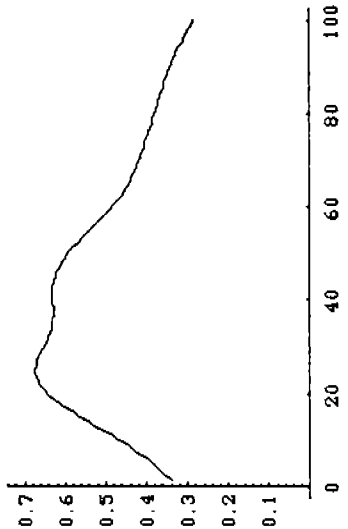
100 pE



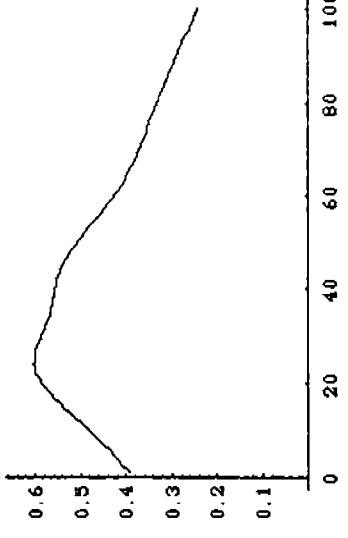
25 pE



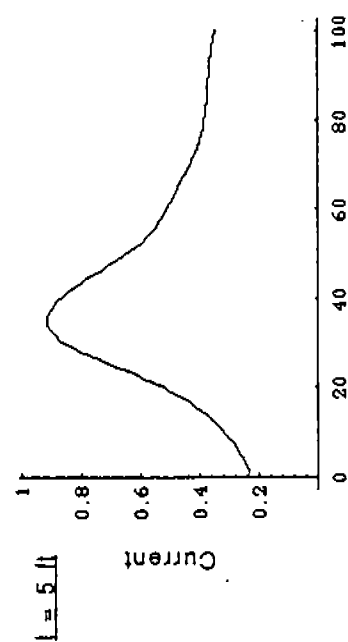
47 pE



100 pE



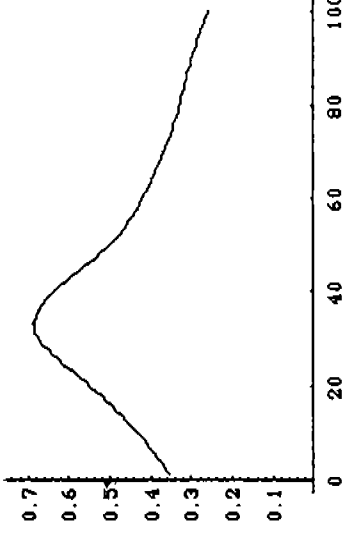
25 pE



47 pE



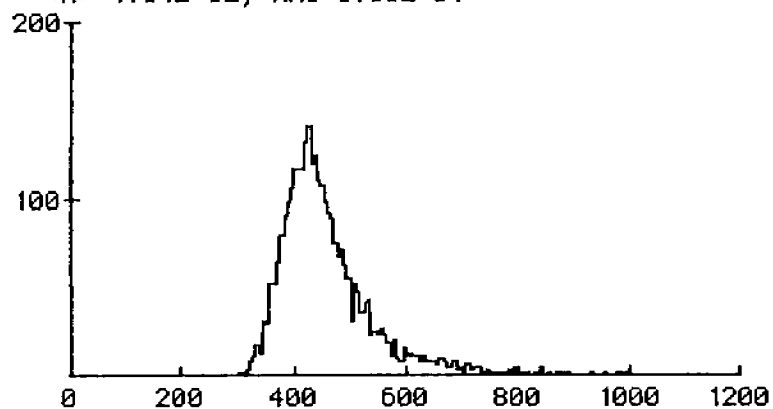
100 pE



ADC L1

N=3068;

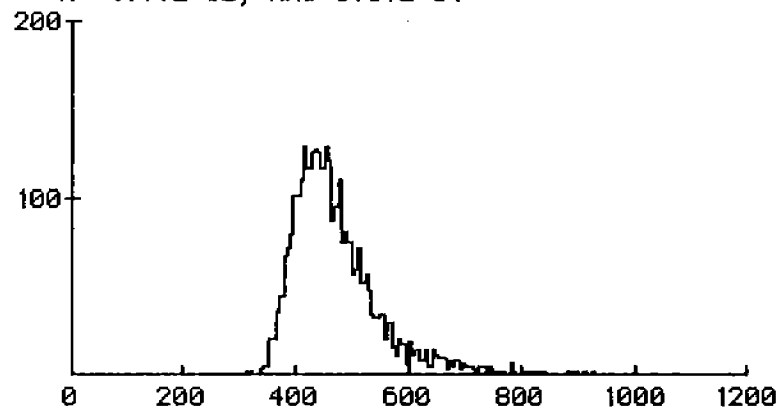
$\langle x \rangle = 4.61E+02$ ; RMS=9.89E+01



ADC R1

N=3068;

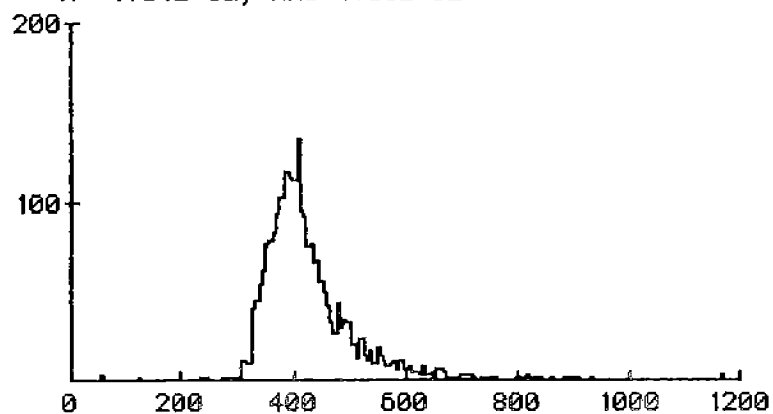
$\langle x \rangle = 4.77E+02$ ; RMS=9.57E+01



ADC L2

N=2508;

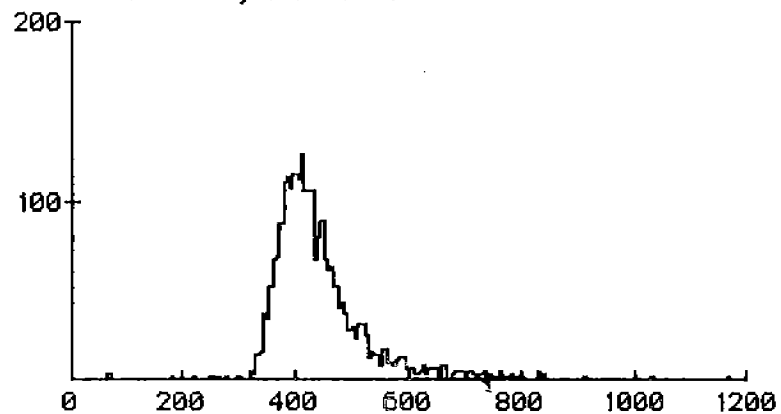
$\langle x \rangle = 4.31E+02$ ; RMS=1.06E+02

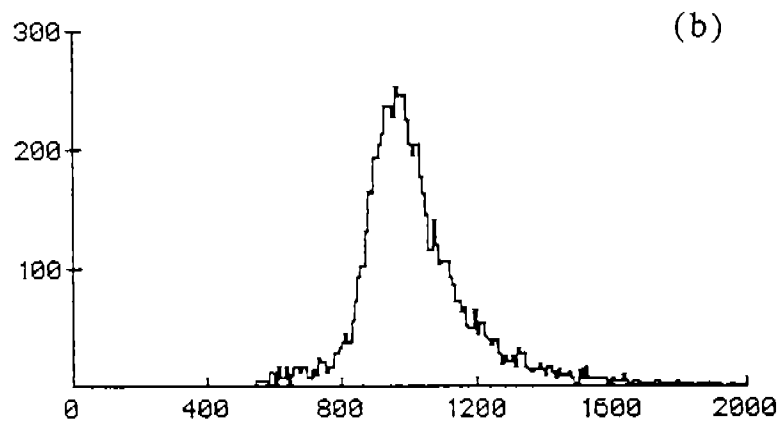
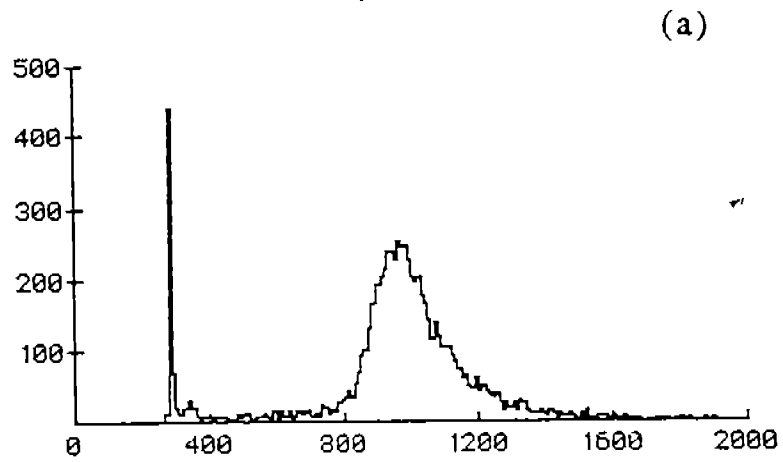


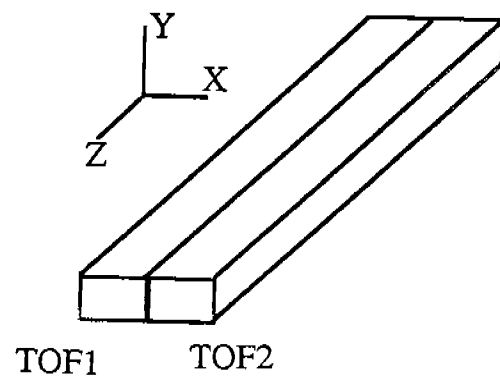
ADC R2

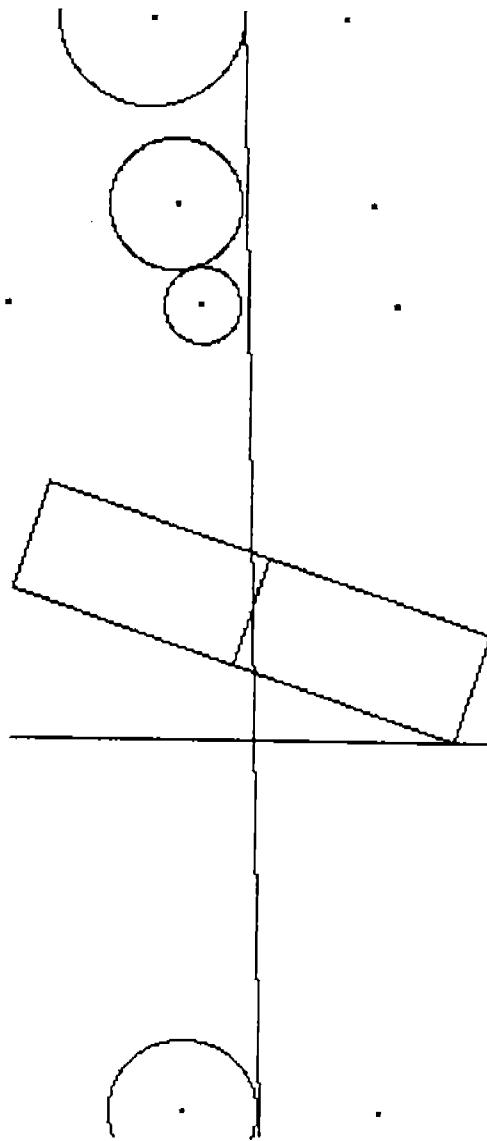
N=2508;

$\langle x \rangle = 4.46E+02$ ; RMS=1.01E+02

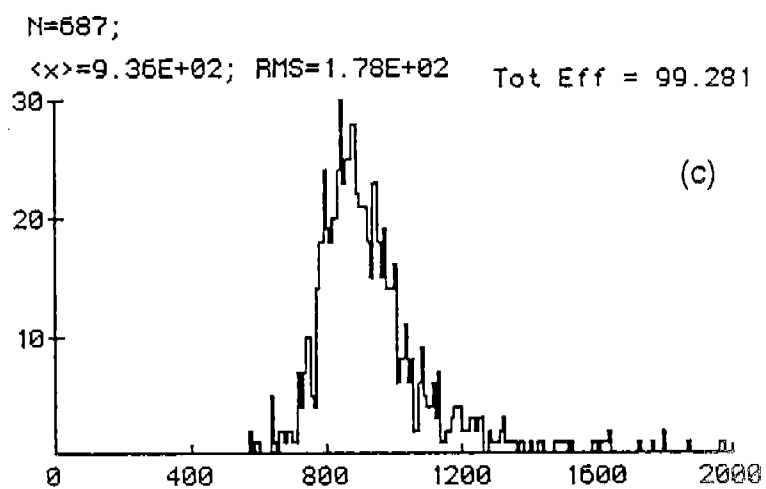
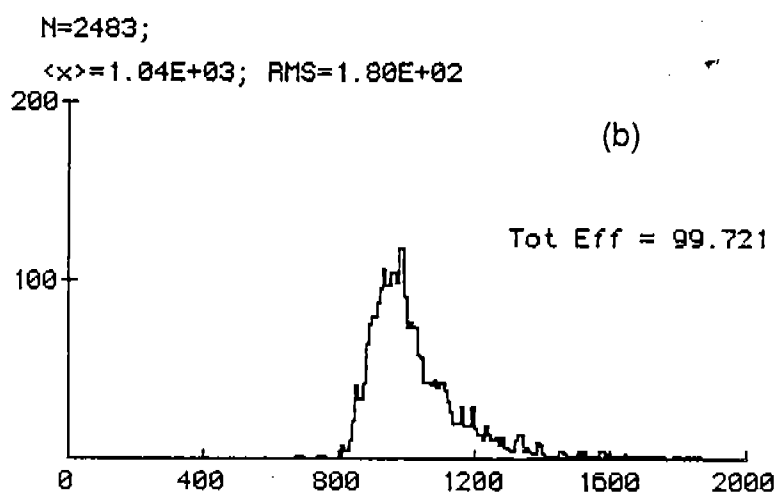
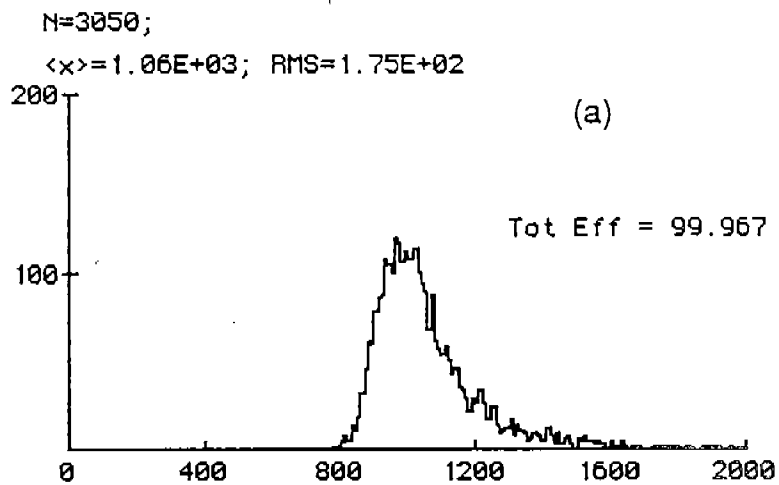








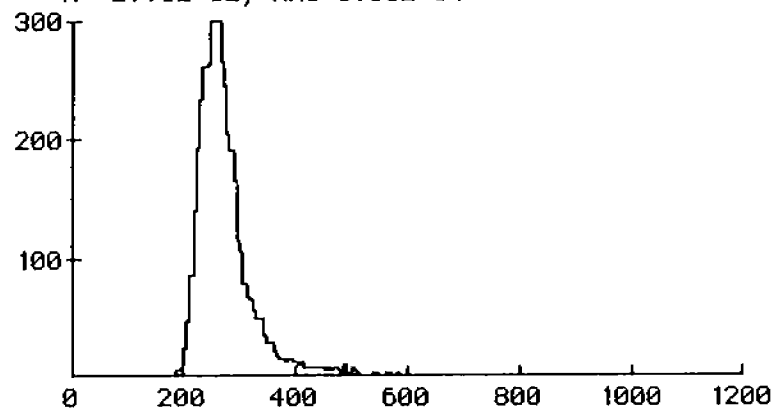




ADC L1

N=4284;

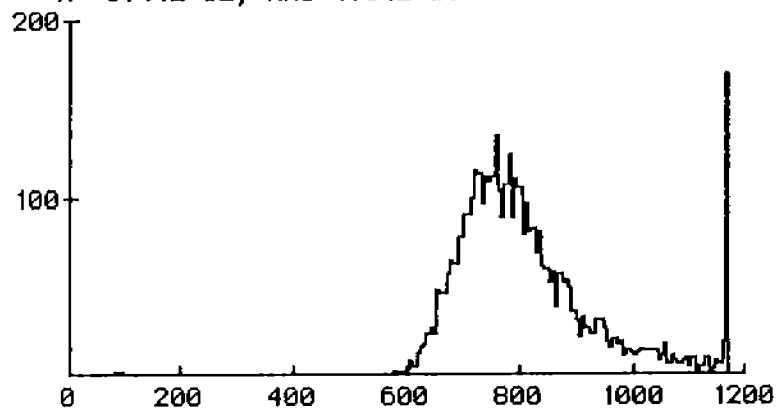
$\langle x \rangle = 2.75E+02$ ; RMS=6.08E+01



ADC R1 1

N=4284;

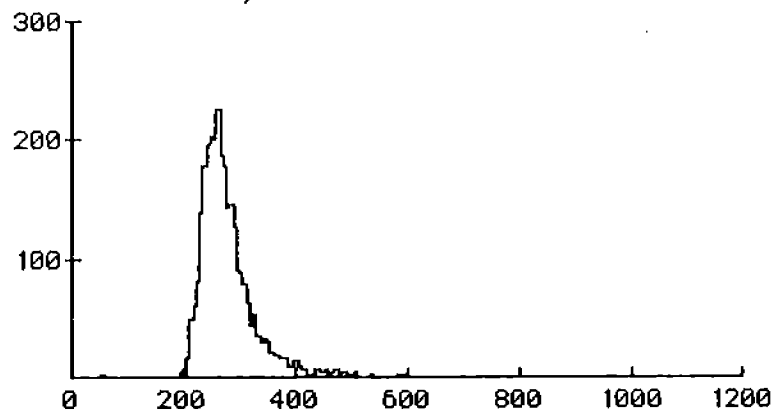
$\langle x \rangle = 8.14E+02$ ; RMS=1.31E+02



ADC L2

N=2955;

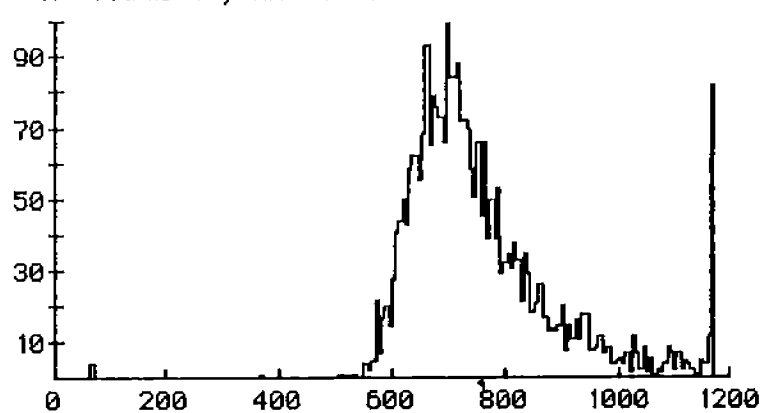
$\langle x \rangle = 2.82E+02$ ; RMS=6.43E+01



ADC R2

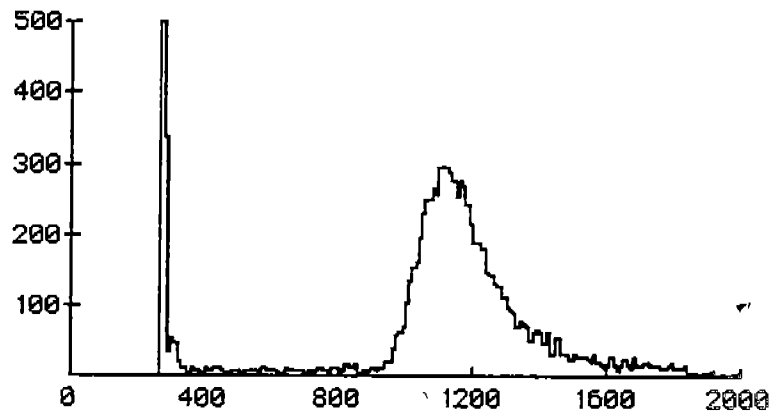
N=2955;

$\langle x \rangle = 7.59E+02$ ; RMS=1.37E+02



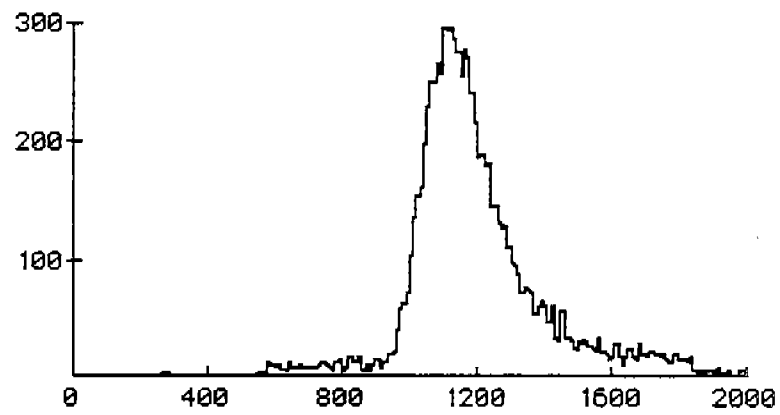
N=10063;

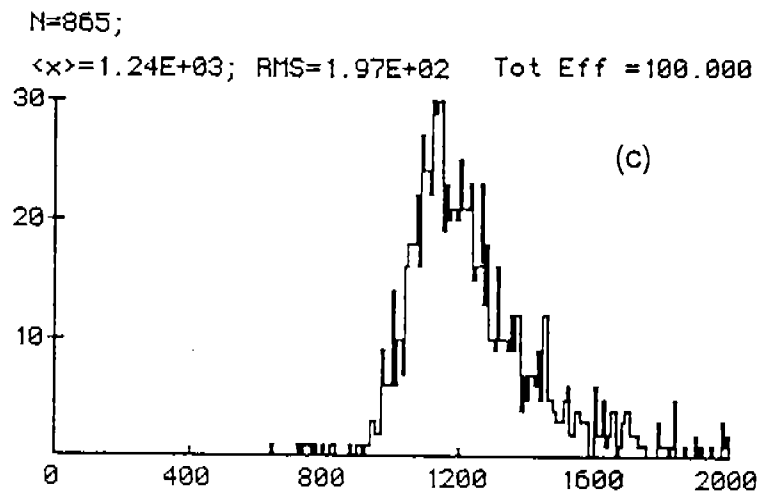
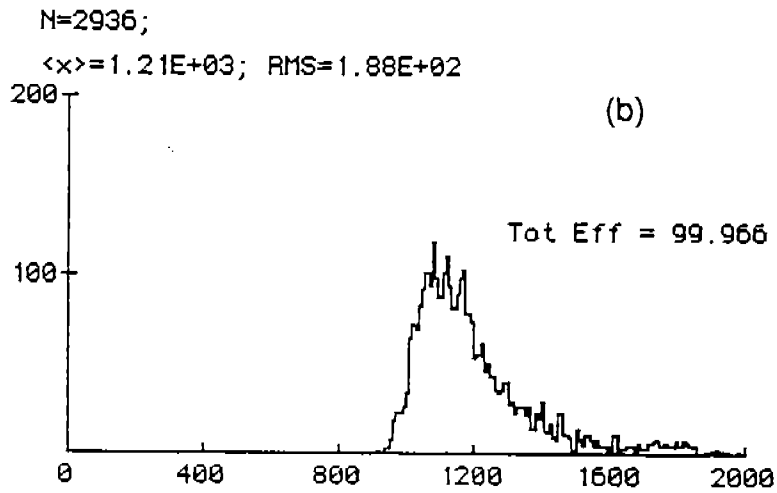
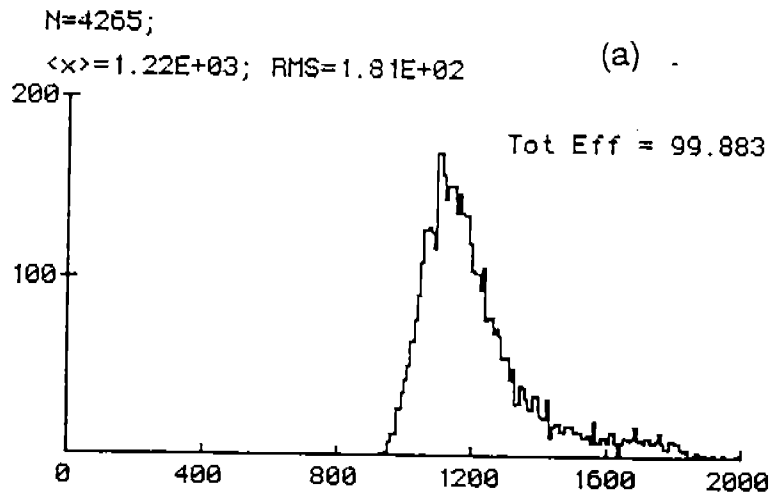
(a)



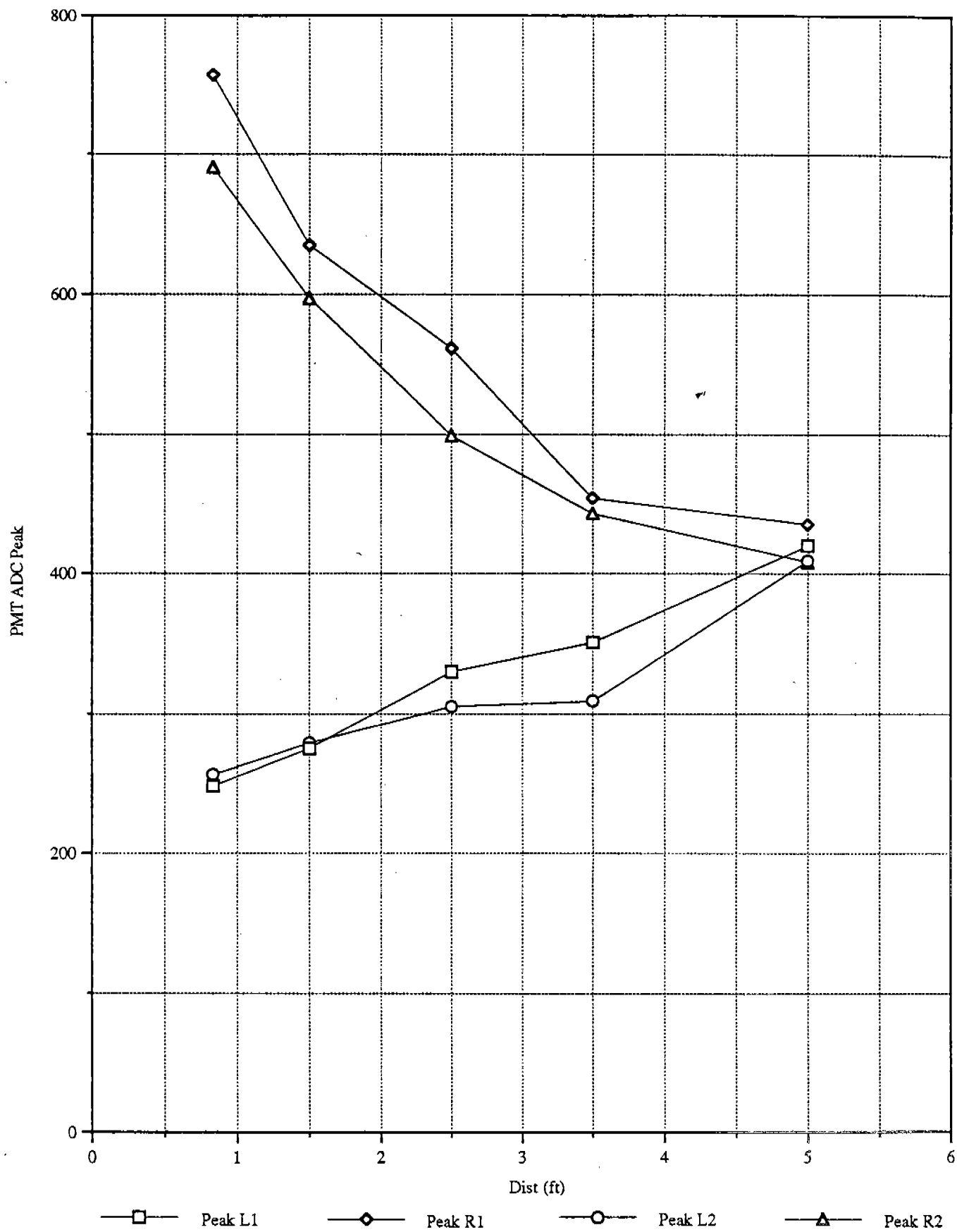
N=8795;

(b)





PMT Peak vs Dist



# Discriminator Histograms at Different Distances

